Int. J. Electrochem. Sci., 11 **(2016)** 5217 – 5225, doi: 10.20964/2016.06.16

International Journal of ELECTROCHEMICAL SCIENCE
www.electrochemsci.org

Multi-Walled Carbon Nanotubes Modified $Li_3V_2(PO_4)_3$/Carbon Composites with Enhanced Electrochemical Performances as Cathode Materials for Li-Ion Batteries

Xiaoyu Cao[1,*], *Peng Ge*[1], *Limin Zhu*[1], *Lingling Xie*[1], *Ziheng Yu*[4], *Jiejie Zhang*[1], *Xiaoli Cao*[2], *Shaoyi Xiong*[3]

[1] School of Chemistry and Chemical Engineering, Henan University of Technology, Zhengzhou 450001, People's Republic of China
[2] School of Electronics and Information Engineering, Sias International University, Zhengzhou 451150, People's Republic of China
[3] Zhengzhou Ruineng Electric Co. Ltd., Zhengzhou 450001, People's Republic of China
[4] No.1 Middle School of Zhengzhou, Zhengzhou 450006, People's Republic of China
[*]E-mail: caoxy@haut.edu.cn

Received: 1 March 2016 / *Accepted:* 8 April 2016 / *Published:* 4 May 2016

The multi-walled carbon nanotubes (MWCNTs) modified $Li_3V_2(PO_4)_3$/carbon composites (MWCNTs-LVPCs) are synthesized through the rheological phase reaction method using MWCNTs as a highly conductive agent. MWCNTs-LVPCs are characterized by X-ray diffraction, scanning electron microscopy, and transmission electron microscope. Charge-discharge cycling performance is also used to characterize the electrochemical properties. X-ray diffraction result reveals that the added MWCNTs do not have a significant effect on the crystal structure of MWCNTs-LVPCs, however, crystal particles growth of MWCNTs-LVPCs are dramatically inhibited by MWCNTs in scanning electron microscopy test. The electrochemical measurements show that the 1.0 wt.%-MWCNTs-LVPC composite yields the highest discharge specific capacity of 182.38 and 163.93 mAh g^{-1} at current rate of 15 and 90 mA g^{-1} among all the MWCNTs-LVPCs, which are much higher than those of $Li_3V_2(PO_4)_3$/carbon composite. After 100 cycles, the 1.0 wt.%-MWCNTs-LVPC composite still maintains a stable capacity of 125.37 mAh g^{-1}. Therefore, construction of MWCNTs modified $Li_3V_2(PO_4)_3$/carbon composites offers an effective and convenient technique to improve the conductivity and electrochemical performances of $Li_3V_2(PO_4)_3$/carbon composites.

Keywords: $Li_3V_2(PO_4)_3$/carbon composites, MWCNTs modification, rheological phase reaction, cathode materials, lithium ion batteries, electrochemical performances

1. INTRODUCTION

Global environmental concerns and the ever-increasing consumption of finite oil resources have stimulated the interest to develop high-rate and high capacity lithium ion batteries (LIBs) for hybrid electric vehicles (HEVs) and electric vehicles (EVs) [1,2]. Recently, the lithium transition metal phosphates such as $LiMPO_4$(M = Co, Mn, Ni, Fe) [3−6] and $Li_3V_2(PO_4)_3$ (LVP) [7] have received intensive attention because of their good thermal stability, high voltage and theoretic capacity. Among them, monoclinic LVP is considered to be a promising cathode materials for LIBs due to its environmental friendliness, low cost, high theoretical capacity, stable crystal structure, and good ion mobility [8−11]. However, the intrinsic poor electronic conductivity (around 2.4×10^{-7} S cm^{-1} at room temperature) of LVP critically limits its practical applications. Therefore, many efforts have been made to overcome the above-mentioned problem including reducing the particle size, coating of carbon and doping metal ions [12−15].

It is well known that MWCNTs have many advantages, such as excellent electronic conductivity [16,17], and it is taken as a novel carbon source exhibiting exceptional electronic and mechanical properties. And recently, the batteries with MWCNTs additives in the electrodes have presented higher total capacity, better high-rate discharge performance and cycle efficiency [16,18]. In our previous work, $Li_3V_2(PO_4)_3$/carbon (LVPC) composites (LVPCs) have been successfully synthesized through the rheological phase reaction (RPR) method, which displays good electrochemical performances [7]. On the basis of this study, graphene decorated LVPCs with improved electrochemical performances have been also prepared via RPR method in our group [19]. Here we describe MWCNTs-LVPCs for use as cathode materials in LIBs prepared by the same process. In comparison with other synthesis methods, the surface area of the solid particles can be utilized efficiently while the contact between solid particle and fluid is close and uniform in the rheological phase system. In these composites, the MWCNTs and LVPC can interlace with each other, which allows fast electron migration and Li^+ ions diffusion and therefore guarantees their high specific capacity and excellent cycling stability.

2. EXPERIMENTAL

MWCNTs-LVPCs were prepared by RPR method similarly as reported in the literatures [7,19−22]. Stoichiometric ratios of $LiOH\cdot H_2O$, V_2O_5, $NH_4H_2PO_4$, $C_6H_8O_7\cdot H_2O$ (citric acid monohydrate) and amount of MWCNTs (0.5 wt.%, 1.0 wt.%, 2.0 wt.%, and 5.0 wt.%; wt.% denotes the mass percentage content of MWCNTs in the target product of MWCNTs-LVPCs) were mixed thoroughly by grinding in an agate mortar. Then the solid-liquid rheological body was fabricated by dropwise adding a proper amount of deionized water. After that, the mixtures in a cylindrical Teflon-lined stainless autoclave were humidified in a blast oven at 80 ^oC for 6 h, and then the MWCNTs-LVPC precursor was obtained by air-drying at 100 ^oC for 12 h. Subsequently, in a tube furnace filled with nitrogen, the precursor was calcined at 350 ^oC for 3 h and then cooled to room temperature. Finally, the calcined materials were ground and calcinated at 800 ^oC for 8 h under the same atmosphere

to produce the MWCNTs-LVPCs (referred to as 0.5 wt.%-MWCNTs-LVPC, 1.0 wt.%-MWCNTs-LVPC, 2.0 wt.%-MWCNTs-LVPC, and 5.0 wt.%-MWCNTs- LVPC, respectively). For the sake of comparison, LVPC was also synthesized under the same conditions but without MWCNTs addition [7]. The mass percentage of carbon content in LVPC was around 14.6 wt.% in this work.

The structural analysis of the LVPC and MWCNTs-LVPCs were performed by the X-ray diffraction (XRD) using a Rigaku X-ray diffractometer system with Cu-Kα radiation source in the 2 θ range of 10^{o}−80^{o}. The morphologies of MWCNTs-LVPCs powders were characterized using JSM-6510LV scanning electron microscope (SEM, JEOL) and Philips Tecnai F20 transmission electron microscope (TEM).

The charge-discharge measurements of the MWCNTs-LVPCs cathodes were implemented by using half-cells assembled in an argon filled glove box (JMS-3, Nanjing Jiumen Automation technology Co., Ltd). The as-obtained active powder was mixed with super P and polytetrafluoethylene microemulsion (PTFE, 60 wt.%) binder (80:10:10 in weight) in isopropanol to form a homogenous slurry, which was pressed into a thick film then onto a porous aluminum mesh. The component of the cells are Li metal as the counter electrode, commercial polyethylene (PE) film as separator (ND420 H129-100), and 1 mol dm^{-3} $LiPF_6$ in Ethylene Carbonate (EC) and Dimethyl Carbonate (DMC) (1:1, v/v) (provided by Guotai-Huarong New Chemical Materials Co., Ltd.) as the electrolyte. The charge-discharge cycles were measured in the 3.0−4.8 V at various current densities and on a multi-channel CT-3008W battery tester (Shenzhen Neware Electronics Co., Ltd.). In order to detect changes in the lattice structure of MWCNTs-LVPCs during cycling, ex-situ XRD was performed at the discharged states of 3.0 V *vs*. Li^+/Li. Fully discharged coin cells were allowed to equilibrate before they were moved to an argon filled glove box where the electrodes were removed from the cells and rinsed with DMC solvent in order to remove any residual salt.

3. RESULTS AND DISCUSSION

Fig. 1 shows the XRD patterns of LVPC and MWCNTs-LVPCs. As shown in Fig. 1, the profiles of the reflection peaks are quite narrow and symmetric. In addition, the added MWCNTs do not have a significant effect on the structure of samples. Otherwise, there are no obvious peaks related to carbon and MWCNTs, which indicates that carbon and MWCNTs are amorphous structure or the amount of them is too low [23−25]. At the same time, the width of Bragg diffraction peaks of MWCNTs-LVPCs is heightened with increasing of the amount of MWCNTs, indicating that MWCNTs can restrict the crystal growth of LVPC.

SEM images of LVPCs containing different weights of MWCNTs are presented in Fig. 2. It can be clearly seen that the particles of LVPCs decrease with the increasing of MWCNTs contents. It is possible that the MWCNTs prevent LVPC crystal particles growth dramatically [26,27]. As well known, smaller grains will lead to shorter transport length for both electrons and Li^+ ions, which are beneficial to both reversible capacity and cycle ability for LVPCs. However, coating the active material with thickly carbon and MWCNTs will lengthen the insertion paths of Li^+ ions, resulting in a much reduce the rate capability of LVPCs. In the consideration of the above situation, we select 1.0

wt.%-MWCNTs-LVPC as a model composite. In order to further investigate the morphology and microstructure of 1.0 wt.%-MWCNTs-LVPC and verify carbon distribution in the composites, TEM images are shown in Fig. 3. It can be found that a fluffy carbon layer is coated on the particle surface of LVP bulk powder, meanwhile, the LVPC particles are well modified by MWCNTs with the thickness of about 155 nm. The dissociative amorphous carbon can link the MWCNTs to the LVP particles effectively, forming a valid conducting network which will leads to excellent electrochemical performances of MWCNTs-LVPCs.

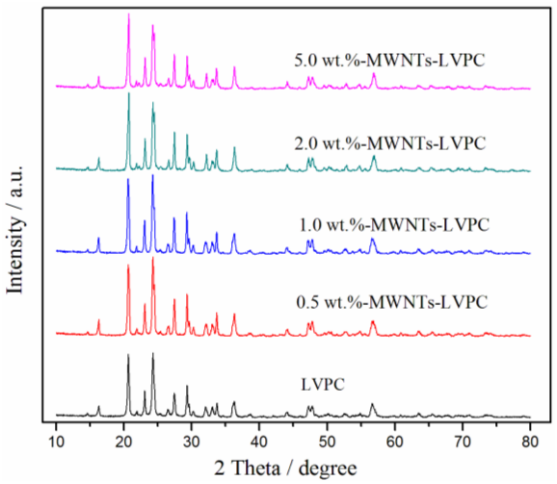

Figure 1. XRD patterns of LVPC and MWCNTs-LVPCs.

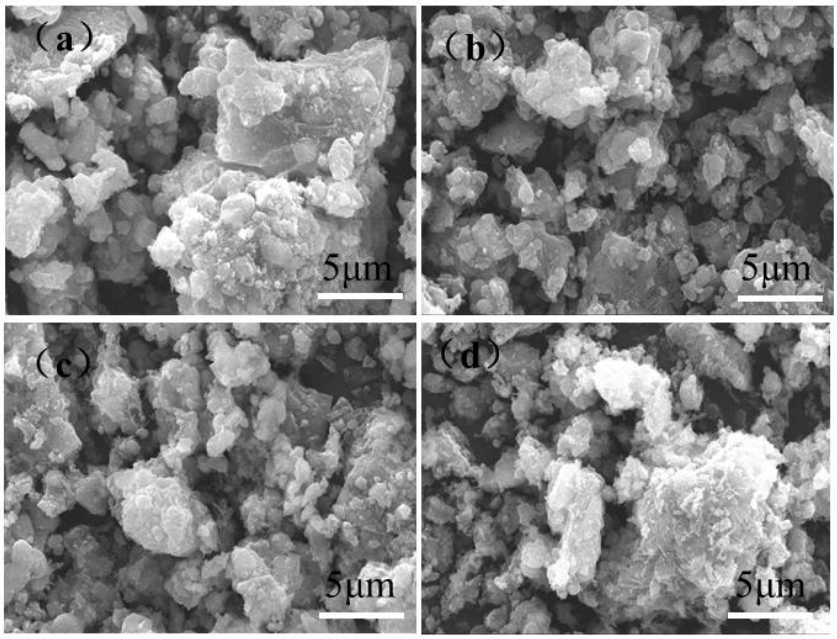

Figure 2. SEM images of LVPCs contained different weights of MWCNTs. 0.5 wt.%-MWCNTs-LVPC (a), 1.0 wt.%-MWCNTs-LVPC (b), 2.0 wt.%-MWCNTs- LVPC (c), 5.0 wt.%-MWCNTs- LVPC (d).

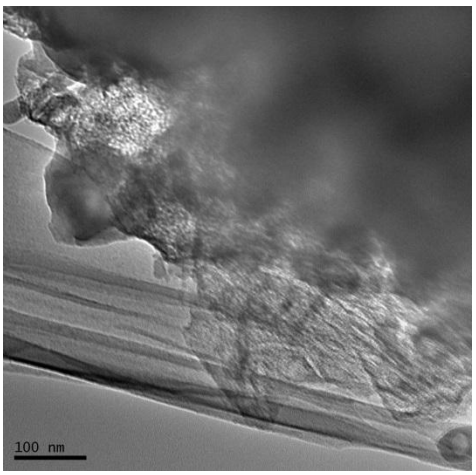

Figure 3. TEM image of 1.0 wt.%-MWCNTs-LVPC.

Fig. 4 (a) exhibits the initial charge-discharge curves of LVPC and MWCNTs-LVPCs in the voltage range of 3.0–4.8 V at the current density of 15 mA g^{-1}. The discharge specific capacities of 0.5 wt.%-MWCNTs-LVPC, 1.0 wt.%-MWCNTs-LVPC, 2.0 wt.%-MWCNTs-LVPC, 5.0 wt.%-MWCNTs-LVPC, and LVPC are 173.17, 182.38, 165.89, 155.22, and 160.39 mAh g^{-1}, respectively. As shown in Fig. 4 (a), 1.0 wt.%-MWCNTs-LVPC almost displays the lowest charge platforms and the highest discharge platforms, and its initial discharge capacities is the highest among all the as-synthesized composites, which may be due to the thickness of the carbon-layer and MWCNTs coating is just right. With increase of the weight of MWCNTs, the 2.0 wt.%-MWCNTs-LVPC and 5.0 wt.%-MWCNTs-LVPC behave lower discharge capacities because of its prolonged diffusion path of Li^+ ions. Fig. 4 (b) shows the cycling performance of all as-prepared composites in the voltage range of 3.0–4.8 V at the current density of 15 mA g^{-1}. It is observed that the discharge specific capacity of 1.0 wt.%-MWCNTs-LVPC remains 135.35 mAh g^{-1} after 100 cycles, demonstrating an excellent cycling stability.

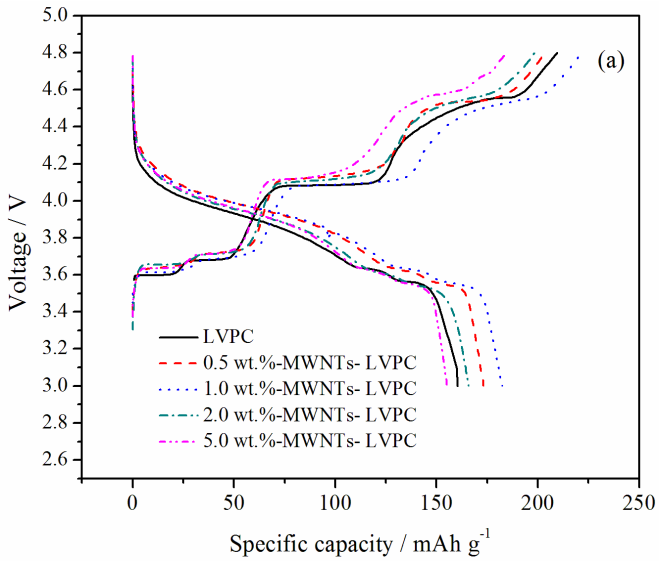

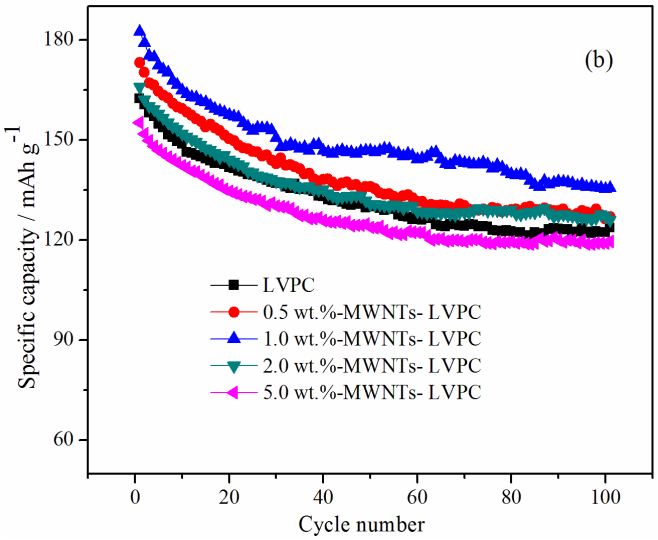

Figure 4. Electrochemical performances of LVPC and MWCNTs-LVPCs in the voltage range of 3.0–4.8 V at the current density of 15 mA g^{-1}. Initial charge-discharge curves (a), cycling performance (b).

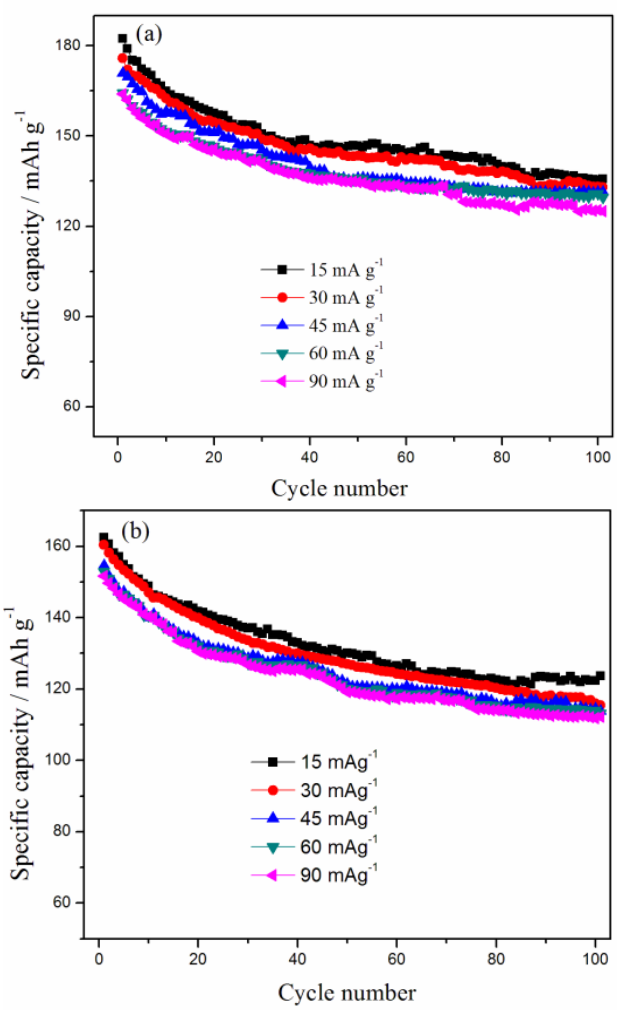

Figure 5. The cycling stability of 1.0 wt.%-MWCNTs-LVPC (a) and LVPC (b) in the voltage range of 3.0–4.8 V at current rates of 15, 30, 45, 60, and 90 mA g^{-1}.

Furthermore, the 5.0 wt.%-MWCNTs-LVPC manifests the lowest capacity, and the results indicate that the amount of added MWCNTs has a remarkable effect on the discharge capacities and cyclic behaviors of LVPCs.

Fig. 5 gives the cycling stability of 1.0 wt.%-MWCNTs-LVPC and LVPC in the voltage range of 3.0–4.8 V at different current densities. It is found that both of them display excellent cyclic performance in all cases, even at a high rate of 90 mA g^{-1} for 100 cycles. But the capacity of 1.0 wt.%-MWCNTs-LVPC is much higher than that of LVPC, and the first discharge capacity of 1.0 wt.%-MWCNTs-LVPC achieves 182.38, 175.87, 170.81,164.32, and 163.93 mAh g^{-1} at the current rates of 15, 30, 45, 60, and 90 mA g^{-1}, respectively. With the current rate increasing, the capacities of both of the two composites gradually decrease in virtue of enhanced electrode polarization. However, the capacities of 1.0 wt.%-MWCNTs-LVPC change less than that of LVPC, when the current rate varies from 15 to 90 mA g^{-1}. The capacity loss of 1.0 wt.%-MWCNTs-LVPC is only 10%, which should be attributed to the novel designed structure: the MWCNTs improve electronic conductivity and prevent the growth of LVPC grains. Moreover, the MWCNTs can form conduct networks to tightly connect the LVPC particles.

To further confirm the excellent reversibility described above, we also carry out an ex-situ XRD characterization of the 1.0 wt.%-MWCNTs-LVPC electrodes after different cycles at the full discharged states and the results are shown in Fig. 6. It can be seen that four 1.0 wt.%-MWCNTs-LVPC electrodes at the 5th, 10th, 15th, and 20th cycle could be indexed to the LVP phase apart from the diffraction pattern of aluminum mesh. However, compared with the repoted ex-situ XRD result [7], the preferred orientation of the diffraction peak has changed when LVPC is combined with MWCNTs. Nevertheless, the four electrodes also display almost same diffraction patterns, suggesting the stable crystal structure during the cycling, which enables the 1.0 wt.%-MWCNTs-LVPC to serve as a conversion electrode with cycling stability and high energy storage capacity.

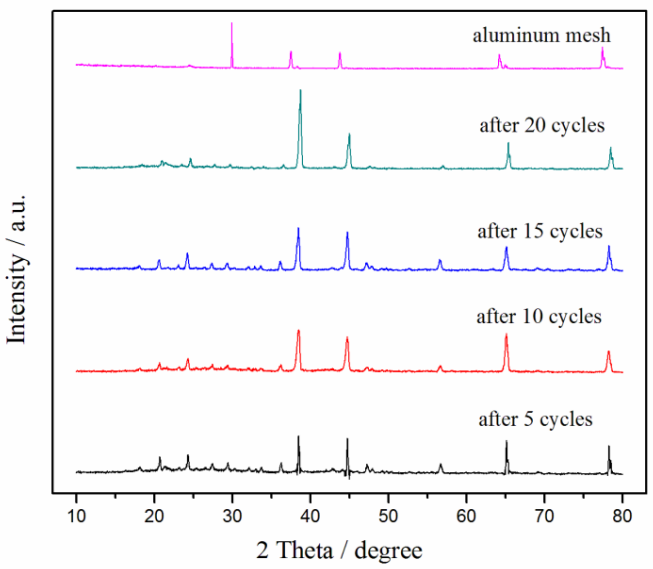

Figure 6. Ex-situ XRD patterns of 1.0 wt.%-MWCNTs-LVPC electrode after different cycles.

4. CONCLUSIONS

In summary, MWCNTs modified LVPCs have been successfully synthesized by RPR method in this work. Compared with the LVPC, the MWCNTs-LVPC composites demonstrate better electrochemical performances, and the improved performances are ascribed to the novel structure. The MWCNTs and the coated-carbon can form a conductive network, facilitating electron migration and Li^+ ions diffusion. The first discharge capacity of 1.0 wt.%-MWCNTs-LVPC could achieve 163.93 mAh g^{-1} at the high current rate of 90 mA g^{-1} and in the voltage range 3.0–4.8 V with faint capacity decay after long cycles and exhibit good high-rate Li^+ ions intercalation/deintercalation properties. This strategy demonstrated in this study offers a convenient and effective technology to design electrode structures for LIBs or other energy storage systems.

ACKNOWLEDGEMENTS
This work was supported by NNSF of China (No. 21403057), Ph.D. Programs Foundation of Henan University of Technology (No. BS150535), Plan for Scientific Innovation Talent of Henan University of Technology, China (No. 2012CXRC09), Fundamental Research Funds for the Henan Provincial Colleges and Universities, China (Nos. 2014YWQN03 and 2015RCJH10), Innovation Scientists and Technicians Troop Construction Projects of Zhengzhou City, China (No. 131PLJRC652).

References

1. M. Armand, J. M. Tarascon, *Nature*, 451 (2008) 652.
2. X. P. Gao, H. X. Yang, *Energ. Environ. Sci.*, 3 (2010) 174.
3. S. Okada, S. Sawa, M. Egashira, J. Yamaki, M. Tabuchi, H. Kageyama, T. Konishi, A. Yoshino, *J. Power Sources*, 97–98 (2001) 430.
4. A. K. Padhi, K.S. Nanjundaswamy, J. B. Goodenough, *J. Electrochem. Soc.*, 144 (1997) 1188.
5. C. Delacourt, P. Poizot, M. Morcrette, J. M. Tarascon, C. Masquelier, *Chem. Mater.*, 16 (2004) 93.
6. X. L. Wu, L. Y. Jiang, F. F. Cao, Y. G. Guo, L. J. Wan, *Adv. Mater.*, 21 (2009) 2710.
7. X. Y. Cao, J. J. Zhang, *Electrochim. Acta*, 129 (2014) 305.
8. Y. Qiao, J. Tu, X. Wang, D. Zhang, J. Xiang, Y. Mai, C. Gu, *J. Power Sources*, 196 (2011) 7715.
9. L. Wang, Z. Tang, L. Ma, X. Zhang, *Electrochem. Commun.*, 13 (2011) 1233.
10. L. Wang, H. Liu, Z. Tang, L. Ma, X. Zhang, *J. Power Sources*, 204 (2012) 197.
11. H. Huang, S. C. Yin, T. Kerr, N. Taylor, L. F. Nazar, *Adv. Mater.*, 14 (2002) 1525.
12. A. Tang, X. Wang, Z. Liu, *Mater. Lett.*, 62 (2008) 1646.
13. J. Su, X. L. Wu, J. S. Lee, J. Kim, Y. G. Guo, *J. Mater. Chem. A*, 1 (2013) 2508.
14. C. Dai, Z. Chen, H. Jin, X. Hu, *J. Power Sources*, 195 (2010) 5775.
15. C. Deng, S. Zhang, S. Yang, Y. Gao, B. Wu, L. Ma, B. Fu, Q. Wu, F. Liu, *J. Phys. Chem., C* 115 (2011) 15048.
16. B. Jin, E. M. Jin, K. H. Park, H. B. Gu, *Electrochem. Commun.*, 10 (2008) 1537.
17. J. Xiang, J. Tu, J. Zhang, J. Zhong, D. Zhang, J. Cheng, *Electrochem. Commun.*, 12 (2010) 1103.
18. X. Li, F. Kang, X. Bai, W. Shen, *Electrochem. Commun.*, 9 (2007) 663.
19. L. Zhu, J. Yang, X. Cao, *Int. J. Electrochem. Sci.*, 10 (2015) 6509.
20. L. Xie, X. Cao, C. Liu, C. Wang, *J. Chil. Chem. Soc.*, 55 (2010) 343.
21. X. Y. Cao, L. J. Guo, J. P. Liu, L. L.Xie, *Int. J. Electrochem. Sci.*, 6 (2011) 27.
22. L. L. Xie, Y. D. Xu, J. J. Zhang, C. P. Zhang, X. Y. Cao, L. B. Qu, *Electron. Mater. Lett.*, 9 (2013) 549.

23. Q. Liu, L. B. Ren, C. J. Cong, F. Ding, F. X. Guo, D. W. Song, J. Guo, X. X. Shi, L. Q. Zhang, *Electrochim. Acta,* 187 (2016) 264.
24. M. Choi, H. S. Kim, Y. M. Lee, W. K. Choi, B. S Jin, *Mater. Lett.,* 160 (2015) 194.
25. R. Y. Zhang, X. Yang, Y. Gao, Y. M. Ju, H. L. Qiu, X. Meng, G. Chen, Y. J. Wei, *Electrochim. Acta,* 188 (2016) 254.
26. S. Q. Chen, Y. Wang, *J. Mater. Chem.,* 20 (2010) 9735.
27. C. L. Zhang, L. F. Shen, H. S. Li, N. Ping, X. G. Zhang, *J. Electroanal. Chem.,* 762 (2016) 1.